Tethys
Journal of Mediterranean Meteorology & Climatology

Tethys 2010, **7**, 57–66
www.tethys.cat
ISSN-1697-1523
eISSN-1139-3394
DOI:10.3369/tethys.2010.7.05
Journal edited by **ACAM**

Measurement and modelling of global erythemal irradiance on inclined planes

D. Serrano[1], **M. J. Marín**[2], **M. P. Utrillas**[1], **F. Tena**[1] **and J. A. Martínez-Lozano**[1]

[1]Solar Radiation Group, Earth Physics and Thermodynamic Department, Universitat de València, Dr Moliner 50, 46100 Burjassot, València

[2]Meteorology-Climatology Laboratory. Mixed Unit CEAM-UVEG. Fundación Centro de Estudios Ambientales del Mediterráneo (CEAM), Charles R. Darwin 14, 46980 Paterna, València

Received: 27-X-2009 – Accepted: 20-II-2010 – **Translated version**

Correspondence to: David.Serrano@uv.es

Abstract

The aim of this paper is the characterization of global erythemal irradiance (UVER) on inclined planes. Different geometric models have been studied, both isotropic and anisotropic, which have been used to estimate the global UVER on inclined planes at 40° in North, South, East and West orientations. This has led to the hypothesis that these models, all of them originally developed to obtain diffuse irradiance in solar spectrum, can be applied in a much more limited range of UVER. The results have been compared with experimental data using the following statistical parameters: mean bias deviation, mean absolute deviation and root mean square deviation. The global UVER was analyzed for all sky conditions and for cloudless sky conditions, and no significant differences were found between the different models in both cases. Overall, the best performing model is Gueymard's anisotropic model, even though it improves the Isotropic model in less than 2%.

Key words: erythemal UV irradiance (UVER), geometric models, UVER on inclined planes, diffuse irradiance

1 Introduction

Erythema or sunburn is the most common of all the effects that UV radiation has in humans. The CIE (*Commission Internationale de l'Éclairage*) adopted in 1987 a standard erythema curve (McKinlay and Diffey, 1987; CIE, 1998) which is commonly used to determine the UV erythemal radiation (UVER). UVER is calculated through the convolution of the spectral curve of the incident radiation at ground level with the curve of the action spectrum proposed by the CIE.

Measurement of the incident erythemal irradiance on horizontal surfaces is not always the most appropriate method to estimate the actual dose received by human beings. For this reason knowledge of the incident irradiance on inclined surfaces can be important for dosimetric studies. Some studies show that the incident global UVER on a plane perpendicular to the sun becomes 27% greater than the incident on a horizontal plane (Parisi and Kimlin, 1999). The influence of topography and ground reflectivity have been studied by Weihs (2002), who obtained that in some specific topographical conditions, the incident intensity on inclined planes may be greater than on horizontal surfaces.

The models used in this study to estimate UVER on inclined planes are geometrical patterns, as they calculate diffuse irradiance divided between various directional components (circumsolar, isotropic part, zenithal, etc..) based on purely geometrical factors and on sky conditions through anisotropy indexes. To model the incident radiation on a non-horizontal plane it is necessary to calculate its direct and diffuse components both reflected as coming from the sky from the UVER irradiance measured on a horizontal plane, namely the global and diffuse components. The main difference between the different geometric models lies in the way of calculating the diffuse sky radiation, as configuration factors and the anisotropy of the sky have to be taken into account. We have assumed that the models originally developed to obtain diffuse irradiance in the solar spectrum can be applied in the UVER spectral range. These models were mostly developed in the 70's and 80's (Utrillas et al., 1991a). We chose the most representative among them, which are also still used in the most recent works (Notton et al., 2006).

Figure 1. Experimental device for measuring diffuse UVER irradiance.

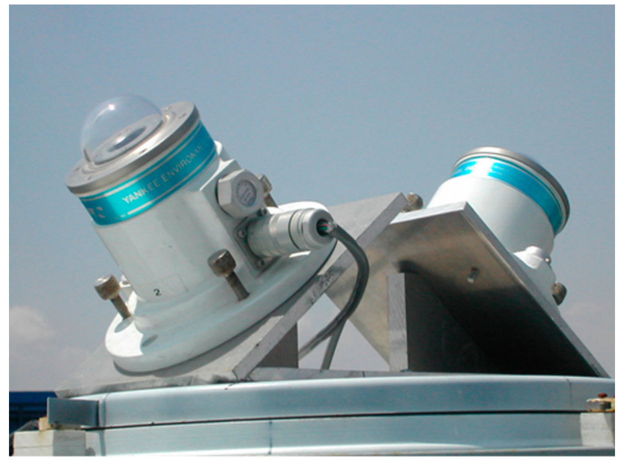

Figure 2. Experimental device for measuring global UVER irradiance on inclined planes.

2 Instrumentation

To study the effects of irradiance on non-horizontal planes, a UVER measurement station was designed and put into operation. The station is located in the Faculty of Physics by the Valencia Solar Radiation Group, and it has four broadband radiometers UVB-1 of Yankee Environmental Systems (YES).

One of them measures the global UVER on the horizontal plane. Another one is coupled with a shadowband anchored in arms whose inclination is equal to the latitude. This band prevents direct sun radiation to reach the detector unit, which makes diffuse irradiance measurements, also in the horizontal plane (Figure 1). The diffuse UVER measurements obtained with the shadowband have been corrected using the modified Batlles model proposed by Utrillas et al. (2007). The corrected experimental values have an uncertainty estimated at 1%.

The other two remaining instruments measure global irradiance on planes inclined at 40°, alternating between North-South and East-West orientations. This last device was built on two premises: a) on the one hand, to measure UVB (280-315 nm) and UVER on inclined planes; b) on the other hand, the radiometers were expected to measure in four azimuthal angles, corresponding to North, South, East and West orientations. The device in Figure 2 was designed to use only two radiometers. The radiometers are inclined at an angle near the latitude of Burjassot (Valencia) (39.5°) which, according to various studies, is the optimum angle to capture maximum radiation on inclined planes (Hartley et al., 1999). Using two timers makes it possible that for the platform to turn every 5 minutes, alternating between both positions.

Consequently, experimental data are recorded every five minutes in UTC time for the instruments in a horizontal position and every ten minutes for those inclined, as ten minutes must pass to resume the same position (Esteve et al., 2006).

The radiometer YES-UVB-1 has a spectral range between 280 to 400 nm and a spectral sensitivity close to the erythema action spectrum. The sensors are calibrated regularly on an annual basis and at two different stages. In the first phase, the sensor that measures global UVER is subjected to a standard calibration and certified at the premises of the National Institute of Aerospace Technology (INTA) (Vilaplana et al., 2006). This calibration consists of measuring the spectral response of the sensor, its angular response to determine the cosine error and a model intercomparison with a Brewer MKIII spectroradiometer outdoors. In the second phase the remaining sensors are calibrated in comparison with the global UVER, which acts as pattern.

This paper presents a statistical analysis of the measurements recorded for about three and half years, from May 2004 until October 2007, together with those modelled for the same period of time with different geometric patterns.

3 Models for calculating UVER radiation on inclined planes

3.1 Total irradiance on an inclined plane

The total irradiance, I_β, received on an inclined plane at an angle of inclination β and an azimuth plane A_p, is calculated as the sum of three terms, direct irradiance, diffuse irradiance reflected by the ground and diffuse irradiance from the sky.

$$I_\beta = I_{b,\beta} + I_{r,\beta} + I_{d,\beta} \tag{1}$$

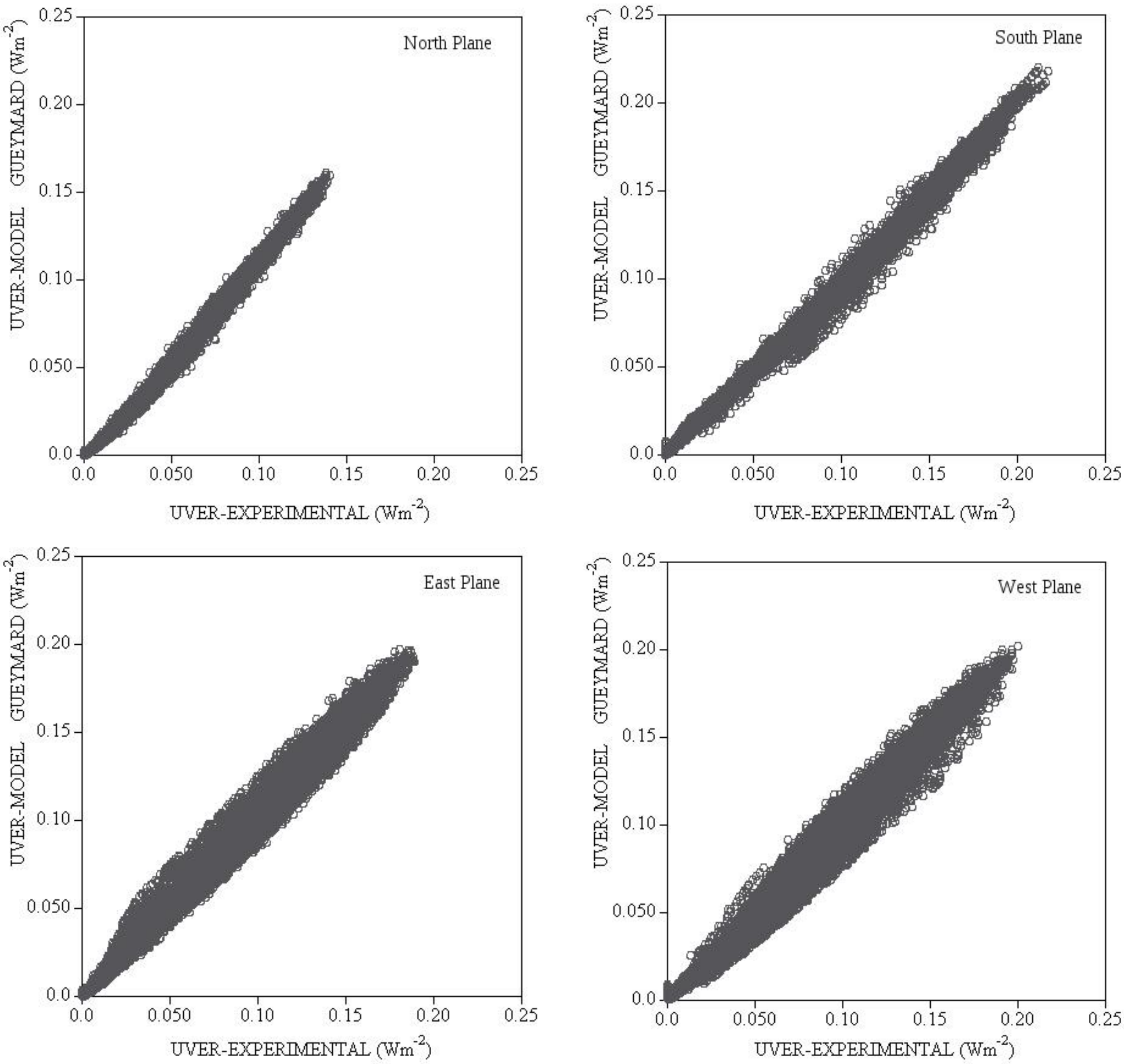

Figure 3. Estimated values with the Gueymard model *vs* experimental values of the global UVER. Planes North, South, East and West.

The first term, corresponding to direct irradiance, is given by the geometric relationship:

$$I_{b,\beta} = I_{b,n} \cos\theta \tag{2}$$

where $I_{b,n}$ is the normal direct erythemal irradiance and θ the solar incidence angle on an inclined plane.

If reflection is considered as isotropic, the diffuse irradiance reflected on the ground will be:

$$I_{r,\beta} = \frac{1}{2}\rho I(1 - \cos\beta) \tag{3}$$

where I is the global erythemal irradiance in a horizontal plane and ρ is the albedo, which for concrete (the ground of the present paper) in the UV has a constant value of 0.1.

Thus the first two components are well defined geometrically, assuming that the ground reflection is isotropic. The diffuse irradiance from the sky is the most difficult to obtain, and this will be the component to be calculated taking into account the different geometric models of radiation described below.

3.2 Isotropic models and pseudo-isotropic models

The diffuse irradiance from the sky is considered uniformly distributed over the entire sky and is representative of overcast conditions. In this case, the diffuse irradiance from the sky is:

$$I_{d,\beta} = \frac{1}{2} I_d(1 + \cos\beta) \tag{4}$$

independent of the azimuth plane and where I_d is diffuse erythemal irradiance on a horizontal plane.

This model, called Isotropic model, was proposed by Liu and Jordan (1962) and underestimates the diffuse component on an inclined plane. The assumption of an isotropic sky for diffuse radiation is not realistic for all sky conditions, as the Southern half of the sky is responsible for 63% of the total diffuse solar radiation from the sky (Hamilton and Jackson, 1985).

Koronakis (1986) amended the assumption of an isotropic diffuse sky, the new expression for the diffuse irradiance becoming:

$$I_{d,\beta} = \frac{1}{3} I_d (2 + \cos\beta) \tag{5}$$

Badescu (2002) also modified the assumption of an isotropic diffuse sky changing some coefficients of the Isotropic model to reach a new expression and obtain acceptable results for different directions simultaneously:

$$I_{d,\beta} = \frac{1}{4} I_d [3 + \cos(2\beta)] \tag{6}$$

3.3 Anisotropic models

3.3.1 Bugler's model

Bugler (1977) added a correction term to the Isotropic model to take into account the diffuse irradiance that comes from the area near the sun and the rest of the sky in accordance with solar elevation:

$$I_{d,\beta} = \frac{1}{2} I_d (1 + \cos\beta) + 0.05 I_{b,\beta} \cdot \cdot \left[\cos\theta - \frac{1}{\cos\theta_z}\left(\frac{1+\cos\beta}{2}\right)\right] \tag{7}$$

where θ_z is the solar zenith angle.

3.3.2 Temps-Coulson's model

Temps and Coulson (1977) introduced two factors in the Liu and Jordan equation (Equation 4) that simulate the anisotropy of the sky in clear conditions, considering the Isotropic model as valid for overcast skies. The first of such correction factors takes into account the diffuse irradiance coming from the circumsolar area, and it is:

$$P_1 = 1 + \cos^2\theta \sin^3\theta_z \tag{8}$$

The second correction factor takes into account the brightness of the sky near the horizon:

$$P_2 = 1 + \sin^3\frac{\beta}{2} \tag{9}$$

The diffuse irradiance from the sky is determined by:

$$I_{d,\beta} = \frac{1}{2} I_d (1 + \cos\beta)\left[1 + \sin^3\frac{\beta}{2}\right] \cdot \cdot (1 + \cos^2\theta \sin^3\theta_z) \tag{10}$$

3.3.3 Hay's model and improved Hay-Willmott model

3.3.3.1 Hay's model

In this model developed by Hay (1979), the diffuse irradiance on an inclined plane is considered to be the addition of the circumsolar component coming from the direction near the solar disk and a diffuse component isotropically distributed from the rest of the sky. These two components are weighted according to an index of anisotropy, F_{Hay}, which represents transmittance through the atmosphere of direct irradiance:

$$F_{Hay} = \frac{I_b}{I_0} \tag{11}$$

where I_b is the direct erythemal irradiance on a horizontal plane and I_0 is the extraterrestrial erythemal irradiance on a horizontal plane.

Then, the diffuse irradiance on an inclined plane is:

$$I_{d,\beta} = I_d\left[F_{Hay}\frac{\cos\theta}{\cos\theta_z} + (1 - F_{Hay})\left(\frac{1+\cos\beta}{2}\right)\right] \tag{12}$$

Clearly, when the diffuse irradiance is close to its global value ($I_d \approx I$), ie on cloudy days, the Hay model is reduced to the Isotropic model.

3.3.3.2 Hay-Willmott model

Willmott (1982) used the same assumptions as Hay and defined a new anisotropic index as:

$$K_\beta = \frac{I_{b,n}}{I_0}\cos\theta \tag{13}$$

now considering the incidence angle instead of the solar zenith angle.

In this model the diffuse irradiance for anisotropic sky will be:

$$I_{d,ani} = \frac{I_d K_\beta}{\cos\theta_z} \tag{14}$$

and diffuse irradiance for an isotropic sky:

$$I_{d,iso} = I_d C_\beta\left(1 - \frac{K_0}{\cos\theta_z}\right) \tag{15}$$

where K_0 is the Willmott anisotropy index for a horizontal surface, being:

$$K_0 = \frac{I_{b,n}}{I_0}\cos\theta_z \tag{16}$$

which coincides with the anisotropy index originally proposed by Hay, F_{Hay}.

The term C_β (Revfeim, 1978) is an isotropic reduction factor for inclined planes:

$$C_\beta = 1.0115 - 0.20293\beta - 0.080823\beta^2 \tag{17}$$

for $0.5 \leq C_\beta \leq 1.0$, with β in radians.

$$I_{d,\beta} = I_d\left[\frac{K_\beta}{\cos\theta_z} + C_\beta\left(1 - \frac{K_0}{\cos\theta_z}\right)\right] \tag{18}$$

3.3.4 Ma-Iqbal model

Ma and Iqbal (1983) propose a model where diffuse irradiance is separated into two terms: a circumsolar one and another that considers the rest of the sky.

The Ma-Iqbal model, unlike the Hay model, used the clearness index as an index of anisotropy:

$$k_t = \frac{I}{I_0} \tag{19}$$

$$I_{d,\beta} = I_d \left[k_t \frac{\cos\theta}{\cos\theta_z} + (1 - k_t) \frac{1 + \cos\beta}{2} \right] \tag{20}$$

3.3.5 Olseth and Skartveit model

Skartveit and Olseth (1986) consider that in case of overcast skies a significant part of the diffuse irradiance comes from the zenith. The authors suggest introducing a correction factor Z as a linear function of the anisotropy index of Hay, F_{Hay}:

$$Z = 0.3 - 2F_{Hay} \tag{21}$$

being $Z = 0$ when $F_{Hay} \geq 0.15$.

$$I_{d,\beta} = I_d \left[F_{Hay} \frac{\cos\theta}{\cos\theta_z} + Z\cos\beta \right] + +I_d \left[(1 - F_{Hay} - Z) \frac{1 + \cos\beta}{2} - S(\Omega_i, \theta_i) \right] \tag{22}$$

where $S(\Omega_i, \theta_i)$ is the portion of solid angle with obstacles on the real horizon. In our case, obstacles on the horizon are virtually nonexistent, and the latter term can be neglected, since the order of magnitude is much smaller than in the other terms.

3.3.6 Gueymard's model

Gueymard (1984, 1986) considers that the irradiance for partially covered skies can be expressed as a linear combination of values between fully covered skies R_{d1} and cloudless skies R_{d0}, which in turn is the addition of the circumsolar component and a hemispheric factor, with the irradiance diffuse:

$$I_{d,\beta} = I_d \left[(1 - N_G) R_{d0} + N_G R_{d1} \right] \tag{23}$$

where N_G is a term that weighs the cloudiness:

$$N_G = \max[\min(Y, 1), 0] \tag{24}$$

with Y as a linear function that depends on $\frac{I_d}{I}$, that is to say, introduces an anisotropic index for measuring the transmittance of the diffused radiation through the atmosphere. Gueymard proposed to determine Y by the expressions:

$$Y = 6.6667 \frac{I_d}{I} - 1.4167 \tag{25}$$

if $\frac{I_d}{I} \leq 0.227$.

$$Y = 1.2121 \frac{I_d}{I} - 0.1758 \tag{26}$$

for the rest of cases.

Irradiance for cloudless skies R_{d0} is calculated as the addition of the circumsolar component and the hemispheric factor:

$$R_{d0} = e^{\left(a_0 + a_1\cos\theta + a_2\cos^2\theta + a_3\cos^3\theta\right)} + F(\beta)G(\gamma) \tag{27}$$

with the a_i coefficients functions of solar elevation, γ.

$$F(\beta) = \frac{1 - 0.2249\sin^2\beta + 0.1231\sin(2\beta)}{1 - 0.2249} - -\frac{0.0342\sin(4\beta)}{1 - 0.2249} \tag{28}$$

$$G(\gamma) = 0.408 - 0.323\gamma' + 0.384\gamma'^2 - 0.170\gamma'^3 \tag{29}$$

with γ' = 0.01γ (γ in degrees).

The irradiance for overcast sky R_{d1} only depends on the inclination angle of the plane and on a correction factor b between the values 1 and 2:

$$R_{d1} = \frac{1 + \cos\beta}{2} - \left(1 + \frac{3}{2b}\right)^{-1} \cdot \cdot \left(\frac{\beta\cos\beta - \sin\beta}{\pi} + \frac{1 - \cos\beta}{2} \right) \tag{30}$$

with β in radians. We will take for b its average value 1.5, as recommended by the author (Gueymard, 1987).

3.3.7 Pérez model

The model of Pérez et al. (1986) is probably the most widely used model in its simplified version (Pérez et al., 1987). This model incorporates the three sub-components to consider: circumsolar diffuse irradiance, horizon diffuse and isotropic diffuse which is determined by two empirically obtained coefficients, F_1 and F_2, called "coefficients of brightness reduction." The expression of the diffuse component on an inclined plane on Pérez model is:

$$I_{d,\beta} = I_d \left[F_1 \frac{a}{b} + (1 - F_1) \frac{1 + \cos\beta}{2} + F_2 \sin\beta \right] \tag{31}$$

The terms a and b are calculated as:

$$a = \max(0, \cos\theta) \tag{32}$$

$$b = \max(\cos 85°, \cos\theta_z) \tag{33}$$

F_1 and F_2 are functions of three variables (θ_z, ε, Δ), that describe the sky conditions, being:

$$\varepsilon = \frac{\frac{I_d + I_b}{I_d} + 1.041\theta_z^3}{1 + 1.041\theta_z^3} \tag{34}$$

$$\Delta = \frac{I_d m}{I_{0,n}} = \frac{I_d}{I_{0,n}\cos\theta_z} \quad (35)$$

where m is the optical mass and ε is the sky clearness index and Δ the sky brightness index of the Pérez model.

F_1 and F_2 are the reduced coefficients of the model that provide the degree of anisotropy, and are calculated according to expressions:

$$F_1 = \max[0, F_{11} + F_{12}\Delta + F_{13}\theta_z] \quad (36)$$

$$F_2 = F_{21} + F_{22}\Delta + F_{23}\theta_z \quad (37)$$

with θ_z in radians.

F_{ij} coefficients were found by a statistical analysis of empirical data for a specific location (Valencia), depending on the value of the sky clearness index, ε (Utrillas and Martínez-Lozano, 1994).

4 Results and discussion

The measurements have been carried out on the Campus of Burjassot (Valencia), which is located at 39.5°N latitude, 0.4°W longitude and 40 m above sea level, where horizon obstacles do not exceed the height of 4°, except for a small band in the Northwest (Esteve et al., 2006). In order to study these models there is a UVER experimental database of over 28,000 ten-minute values for solar zenith angles below 70°, thus avoiding high cosine errors for each of the four planes, North, South, East and West.

In order to assess the goodness of fit of the different models, the following statistical parameters have been used: mean bias deviation (MBD), mean absolute deviation (MAD) and root mean square deviation (RMSD), which indicate the deviation between the experimental values and those estimated by the models, being the expressions of these parameters (Willmott and Matsuura, 2005):

$$MBD = \frac{\sum_{i=1}^{N}(y_i - x_i)}{N\bar{x}} \quad (38)$$

$$MAD = \frac{\sum_{i=1}^{N}|y_i - x_i|}{N\bar{x}} \quad (39)$$

$$RMSD = \frac{\left[\frac{\sum_{i=1}^{N}(y_i - x_i)^2}{N}\right]^{1/2}}{\bar{x}} \quad (40)$$

where y_i is the i-th estimated value, x_i the i-th measured value, $\bar{x}$ the mean measured value and N the number of total data analyzed.

The RMSD statistic parameter gives the points which are furthest from the mean value greater weight than MAD, however Willmott and Matsuura (2005) recommend the use of MAD as an evaluation of average error. They always have positive values. By contrast, the MBD is the difference between the estimated and experimental value, corresponding to an overestimation or underestimation of the experimental values by the model (Utrillas et al., 1991b). Relative values have been taken for all statistical indicators in order to facilitate comparison.

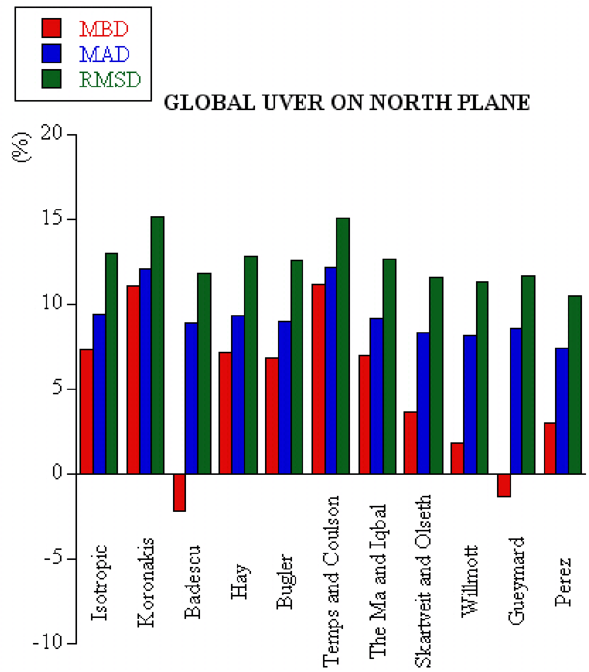

Figure 4. Mean bias deviation (MBD), mean absolute deviation (MAD) and root mean square deviation (RMSD), which indicate the relative deviation between experimental values and those estimated by all models presented in this paper for the North orientation.

Figure 3 shows, as an example, the estimated values by the anisotropic model of Gueymard, as it is the model that provides the best results in Valencia for the four orientations compared with experimental values. In this figure we can see the low dispersion that occurs at the North plane and the high dispersion found both in the East and the West orientations. It is also noted that the highest values are recorded in South orientation.

4.1 Overall UVER on inclined surfaces for all sky conditions

Figure 4 shows the results for the plane North, which is the plane on which we receive less irradiance of the four orientations studied. The relative MBD statistic parameter shows that all models, except the pseudo-isotropic of Badescu and the anisotropic of Gueymard, overestimate the experimental values, with the Koronakis and Temps-Coulson models as the ones that most overestimate the experimental measurements, with values approaching 11%. Regarding the relative MBD statistic parameter, none of the studied models exceed 10% except the models of Koronakis and Temps-Coulson with values of 12%. The model that provides the best result is that of Pérez, with 7%, which enhances the

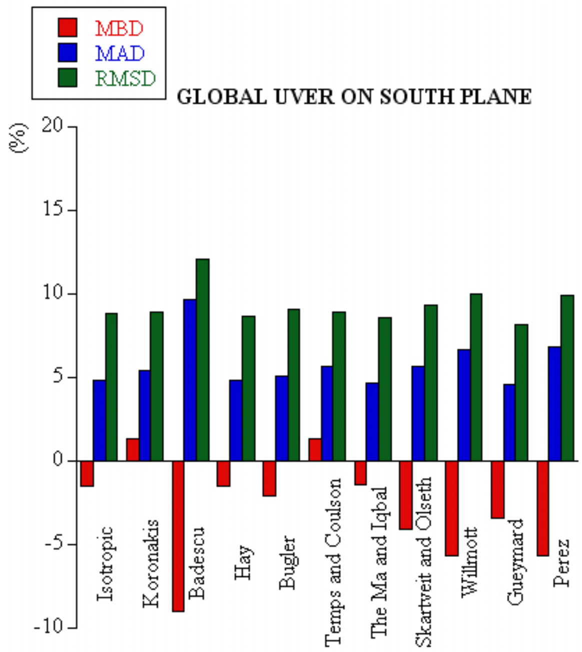

Figure 5. As in Figure 4 for the South orientation.

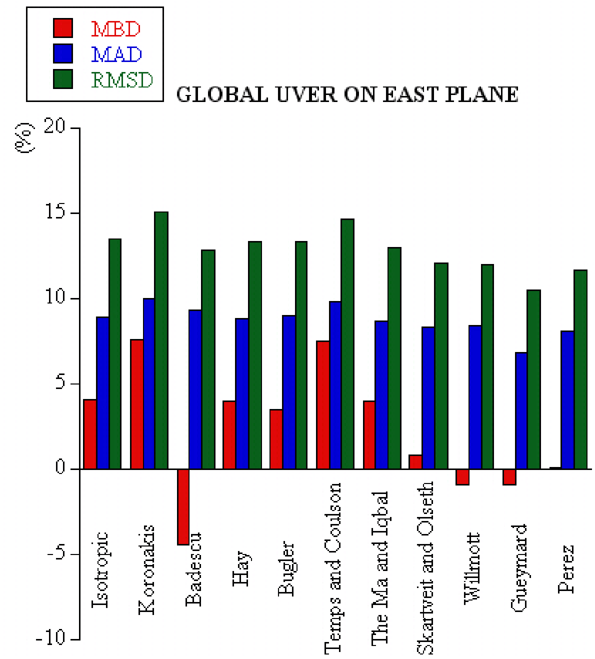

Figure 6. As in Figure 4 for East orientation.

Isotropic model by 2%. Regarding the relative RMSD statistic parameter, none of the models are over 16%, and most of them provide values below 13%, being the model of Pérez, again, the one that provides the best result with 11%. The most unfavorable models are those of Koronakis and Temps-Coulson with values above 15%.

The best results from all planes of different inclination studied are found in the South oriented plane (Figure 5). This orientation receives the greatest irradiance during the day and it is where direct radiation plays a more important role. Also noteworthy is that most models have been developed initially for this orientation. The relative MBD shows that most models underestimate the experimental values, except for in the Koronakis and Temps-Coulson models, which overestimate them, with values below 2%. As for relative MAD, on the South plane the results obtained are the lowest of the orientations considered, with values below 10% even in the worst case, Badescu's model. Most models provide a relative MAD between 5% and 6%, which is comparable to the uncertainty of experimental measurements, which is 5-6%. In turn, the relative RMSD provides values below 13%, between 9% and 10% for most models. Therefore, except for Badescu's model, which underestimates the results in excess, all models performed well, being the Gueymard's model the one that provides the best results, but improving the Isotropic model in less than 1%.

East and West planes get the same irradiance throughout the day, therefore the results found are similar for the different statistical parameters studied, as shown in Figures 6 and 7 respectively. The relative MBD shows that on the East oriented plane most of the models overestimate the experimental values (generally less than 5%) except for the three models that underestimate it. For the West oriented plane, half of the models overestimate the experimental values and the other half underestimate them, all below 5%, except Badescu's model, which underestimates them by 7%. For the MAD the two inclinations have very similar values, below 10%, the Gueymard's model being the one that provides the best result with a value less than 7% in both cases. With regard to RMSD, the two planes provide values below 16%, and in general the values obtained for the West plane are slightly lower than those obtained for the East plane. Again, the Gueymard's model provides a better result, with a value of 11% in the two planes.

The Gueymard's model has the best results for all directions except the North, which is enhanced by the Pérez model, although this improvement is only 1%. It should be noted that no model, including that of Gueymard or Pérez, significantly improves the Isotropic model, which showed a discrepancy regarding them below 2% for all orientations.

4.2 Global UVER on inclined surfaces for cloudless skies

The study was repeated taking only the experimental values of cloudless sky conditions. To select the data, the modified clearness index $k_{t'}$ was used, which has the advantage over the clearness index of reducing dependence on solar zenith angle and is defined as (Pérez et al., 1990):

$$k_{t'} = \frac{k_t}{1.031e^{-1.4/(0.9+9.4/m)} + 0.1} \qquad (41)$$

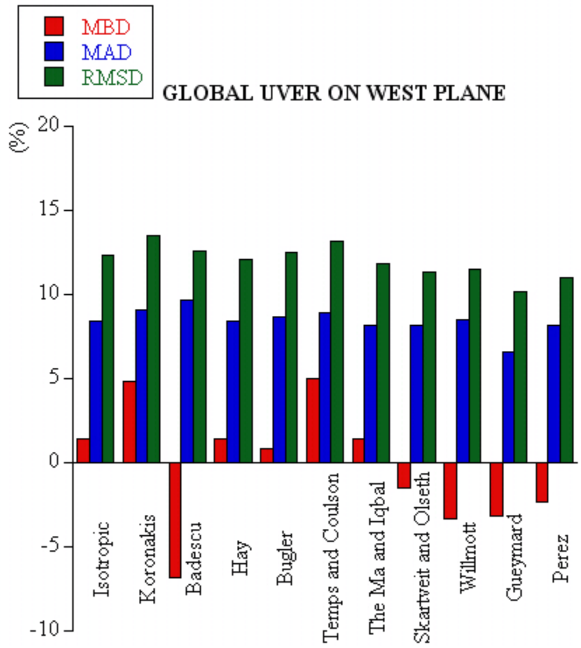

Figure 7. As in Figure 4 for West orientation.

where k_t is the clearness index (Equation 19) and m is the optical mass.

Figure 8 shows the percentage of $k_{t'}$ values obtained for Burjassot (Valencia). The figure was obtained with the values of the measurements taken during three and a half years. From it we can conclude that in Valencia there is a predominance of cloudless skies since the highest percentages of the clearness index are in the intervals between 0.6 and 0.8. A value of the modified clearness index higher than 0.7 was adopted as a criterion to identify clear-sky conditions. After selecting the values of cloudless skies, the analysis of MBD, MAD and RMSD were repeated for each geometric model studied earlier.

To the North and East directions all models show a positive relative MBD, overestimating the experimental values, except Badescu's model at the East plane. In contrast, to the South and West directions all the models underestimate it, except those of Koronakis and Temps-Coulson at the South plane. Regarding the relative MAD and RMSD statistical parameters, the models give worse results with respect to considering all sky conditions, for orientations North, East and West. The same applies for the South plane, except for Koronakis and Temps-Coulson models, which slightly improve the results.

In general, for all orientations errors are higher than those obtained when we considered all sky conditions. This is because these models were originally developed for the entire bandwidth of the solar spectrum where the diffuse component is only 10% of the total irradiance (Martínez-Lozano et al., 1994), in contrast to the UVER range the diffuse component on clear days gets to values of 60% (Utrillas et al., 2007); therefore the conditions of anisotropy do not correspond to the predictions of the models.

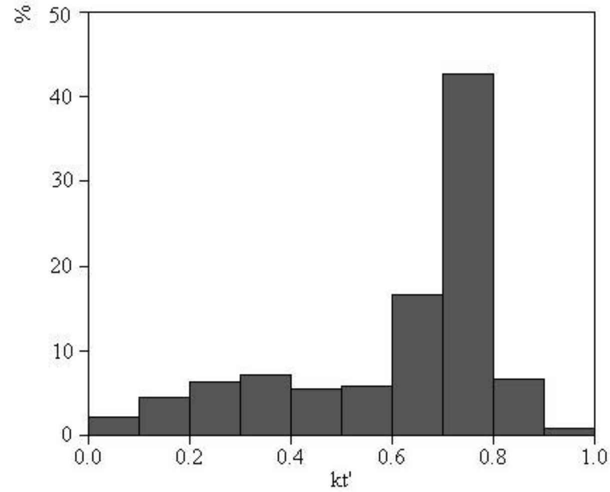

Figure 8. Percentage of the modified clearness index for Burjassot (Valencia).

The results get between 1% and 2% worse for the Isotropic model, and less than 1% for the Gueymard's model. This means that the studied models behave better in the event of cloudy skies than considering only conditions of cloudless skies. However, at the South plane the Koronakis and Temps-Coulson models improve the outcomes by 2%, as they were originally developed for cloudless skies.

5 Conclusions

In this work we calculated the global UVER using geometric models and experimental measurements for planes inclined 40° and directions North, South, East and West have been compared to them. To assess the results the relative MBD, MAD and RMSD statistical parameters were analyzed.

Using the UVER values for all sky conditions, the values of the relative MBD show that almost all models overestimate the experimental values for the North direction, while for the South orientation, most of the models underestimate them. For the East and West orientations, with the exception of Badescu, Koronakis and Temps-Coulson models, the models overestimate or underestimate the results below 5%.

All the models analyzed satisfactorily reproduce the global UVER on the South plane with a MAD at about 5%, while on the other planes higher discrepancies are obtained, at about 9%. On the South plane the RMSD values are approximately 9%, between 11% to 15% on the other planes. Gueymard's model provides the best results for all directions except the North, in which the Pérez model provides better results. However, no model in any direction improves the results provided by the Isotropic model by more than 2%. After analyzing the different planes of incidence, we observed that for each orientation different models present the best results, although the difference between them is not significant.

To analyze the influence of cloudiness on UVER modeling on inclined planes, the previous study was repeated considering only the condition of cloudless skies, which was selected by a modified clearness index value ($k_{t'}$) higher than 0.7. Analyzing the values of $k_{t'}$ for Burjassot (Valencia) in the period considered in this study, we conclude that there is a predominance of cloudless skies, as 65% of cases have a $k_{t'}$ higher than 0.6.

The analysis of MBD in the case of cloudless sky conditions shows that in the North orientation the models overestimate the experimental values more than in the previous case, while for the South orientation the underestimation is also greater. Regarding the East and West directions the results are similar to the case of all sky conditions. Regarding the relative MAD and RMSD, the results are worse than when all sky conditions are considered for the North, East and West orientations. For the South orientation the results are worse in the case of cloudless skies, except for those obtained with the Koronakis and Temps-Coulson models. It should be noted that these models were developed for these cloudless sky conditions.

In general, for all orientations, the errors obtained when considering only cloudless skies are higher than those obtained when considering all sky conditions. Gueymard's model is the exception because it includes a cloudiness factor, and therefore it works properly both with overcast and cloudless skies.

To improve these results, these models should be adapted in order to minimize the errors obtained, especially for planes different than South, which are the orientations where larger discrepancies are registered. Another aspect to improve is to avoid the underestimation of the models, which mainly occurs on the South plane, by recalculating the anisotropy factors, defining a new specific clearness index in the UVER range, which would be representative of the greater weight of the diffuse component in that range with respect to the total irradiance.

Acknowledgements. This work was funded by the Ministry of Science and Innovation (MICINN) through the projects "GRACCIE (CSD2007-00067, Programme CONSOLIDER-INGENIO 2010) and CGL2007-60648, together with the European Social Fund through the "Torres Quevedo" contract of M. J. Marín. The CEAM Foundation is supported by the *Generalitat Valenciana* and Bancaixa.

Appendix A Nomenclature

- a_0, a_1, a_2, a_3: Gueymard's model coefficients.
- F, G: Gueymard's model functions.
- F_{Hay}: index of anisotropy of the Hay's model.
- F_1, F_2: reduced brightness functions of the Pérez model.
- I: global erythemal irradiance on a horizontal plane.
- I_β: global erythemal irradiance on an inclined plane β.
- I_b: direct erythemal irradiance on a horizontal plane.
- $I_{b,n}$: normal direct erythemal irradiance.
- $I_{b,\beta}$: direct erythemal irradiance for an inclined plane β.
- I_d: diffuse erythemal irradiance on a horizontal plane.
- $I_{d,ani}$: anisotropic diffuse erythemal irradiance.
- $I_{d,iso}$: isotropic diffuse erythemal irradiance.
- $I_{d,\beta}$: diffuse erythemal irradiance on a slope β.
- $I_{r,\beta}$: reflected erythemal irradiance on an inclined plane β.
- I_0: extraterrestrial erythemal irradiance on a horizontal plane.
- K_β: index of anisotropy of the Hay and Willmott model.
- N_G: term that weighs the clouds, Gueymard's model.
- P_1, P_2: Temps and Coulson model parameters.
- R_{d0}: Gueymard coefficient for cloudless skies.
- R_{d1}: Gueymard coefficient for cloudy skies.
- Y: Gueymard's atmospheric transmittancv function.
- Z: Skarveit and Olseth model correction factor.
- γ: solar elevation.
- A_p: azimuth plane.
- m: optical mass.
- Δ: Pérez model sky brightness index.
- ε: Pérez model sky clearness index.
- $k_{t'}$: clearness index modified.
- β: inclination of the plane.
- θ: solar incidence angle on an inclined plane.
- θ_z: solar zenith angle.
- ρ: albedo.
- Ω: solid angle.

References

Badescu, V., 2002: *3D isotropic approximation for solar diffuse irradiance on tilted surfaces*, Renew Energy, **26**, 221–223.

Bugler, J. W., 1977: *The determination of hourly insolation on an inclined plane using a diffuse irradiance model based on hourly measured global horizontal insolation*, Sol Energy, **19**, 477–491.

CIE, 1998: Erythema reference action spectrum and standard erythema dose, Vienna, ISO 17166:1999/CIE S007-1998.

Esteve, A. R., Marín, M. J., Martínez-Lozano, J. A., Tena, F., Utrillas, M. P., and Cañada, J., 2006: *UV index on tilted surfaces*, Photochem Photobiol, **82**, 1047–1052.

Gueymard, C., 1984: Physical modelling of the diffuse irradiance on tilted planes as a function of the aerosols anisotropic effect, Meteorology and renewable energies conference, AFME, Valbonne, France, pp. 303-314.

Gueymard, C., 1986: Radiation on tilted planes: A physical model adaptable to any computational time-step, Proceedings of INTERSOL85, Elmsford, NY: Pergamon Press, pp. 2463-2467.

Gueymard, C., 1987: *An anisotropic solar irradiance model for tilted surfaces and its comparison with selected engineering algorithms*, Sol Energy, **38**, 367–386.

Hamilton, H. L. and Jackson, A., 1985: *A shield for obtaining diffuse sky radiation from portions of the sky*, Sol Energy, **34**, 121–

123.

Hartley, L. E., Martínez-Lozano, J. A., Utrillas, M. P., Tena, F., and Pedrós, R., 1999: *The optimisation of the angle of inclination of a solar collector to maximise the incident solar radiation*, Renew Energy, **17**, 291–309.

Hay, J. E., 1979: Study of shortwave radiation on non-horizontal surfaces, Atmospheric Environment Service, Downsview, Ontario, rep. 79-12.

Koronakis, P. S., 1986: *On the choice of the angle of tilt for south facing solar collectros in the Athens basin area*, Sol Energy, **36**, 217–225.

Liu, B. Y. H. and Jordan, R. C., 1962: *Daily insolation on surfaces tilted towards the equator*, Trans ASHRAE, pp. 526–541.

Ma, C. C. Y. and Iqbal, M., 1983: *Statistical comparison of models for estimating solar radiation on inclined surfaces*, Sol Energy, **31**, 313–317.

Martínez-Lozano, J. A., Utrillas, M. P., and Gómez, V., 1994: *Estimation of the diffuse solar irradiation from global solar irradiation. Daily and monthly average daily values*, Renew Energy, **4**, 95–100.

McKinlay, A. F. and Diffey, B. L., 1987: *A reference spectrum for ultraviolet induced erythema in human skin*, CIE Journal, **6**, 17–22.

Notton, G., Cristofari, C., and Poggi, P., 2006: *Performance evaluation of various hourly slope irradiation models using Mediterranean experimental data of Ajaccio*, Energy Conv Manag, **47**, 147–173.

Parisi, A. V. and Kimlin, M. G., 1999: *Horizontal and sun-normal spectral biologically effective ultraviolet irradiances*, J Quant Spectrosc Radiat Transf, **35**, 151–158.

Pérez, R., Stewart, R., Arbogast, R., Seals, J., and Scott, J., 1986: *An anisotropic hourly diffuse radiation model for surfaces: description, performance validation, site dependency evaluation*, Sol Energy, **36**, 481–497.

Pérez, R., Stewart, R., Ineichen, R., Seals, J., and Menicucci, D., 1987: *A new simplified version of the Perez diffuse irradiance model for tilted surfaces*, Sol Energy, **39**, 221–231.

Pérez, R., Ineichen, P., Seals, J., and Zelenka, A., 1990: *Making full use of the clearness index for parametering hourly insolation conditions*, Sol Energy, **45**, 111–114.

Revfeim, K. J. A., 1978: *A simple procedure for estimating global daily radiation on any surface*, J Appl Meteorol, **5**, 1126–1131.

Skartveit, A. and Olseth, J. A., 1986: *Modelling slope irradiance at high latitudes*, Sol Energy, **36**, 333–344.

Temps, R. C. and Coulson, K. L., 1977: *Solar radiation incident upon slopes of different orientation*, Sol Energy, **19**, 179–184.

Utrillas, M. P. and Martínez-Lozano, J. A., 1994: *Performance evaluation of several versions of the Perez tilted diffuse irradiance model*, Sol Energy, **53**, 155–162.

Utrillas, M. P., Martínez-Lozano, J. A., and Casanovas, A. J., 1991a: *Evaluation of models for estimating solar irradiation on vertical surfaces at Valencia, Spain*, Sol Energy, **47**, 223–229.

Utrillas, M. P., Martínez-Lozano, J. A., and Casanovas, A. J., 1991b: *Desviaciones entre valores estimados y experimentales de irradiancia global y difusa sobre superficies verticales*, Opt Pura Apl, **24**.

Utrillas, M. P., Marín, M. J., Esteve, A. R., Tena, F., Cañada, J., Estellés, V., and Martínez-Lozano, J. A., 2007: *Diffuse UV erythemal radiation experimental values*, J Geophys Res, **112**, D24 207.

Vilaplana, J., Cachorro, V., Sorribas, M., Luccini, E., de Frutos, A., Berjón, A., and de la Morena, B., 2006: *Modified calibration procedures for a Yankee Environmental System UVB-1 biometer based on spectral measurements with a Brewer spectrophotometer*, Photochem Photobiol, **82**, 508–514.

Weihs, P., 2002: *Influence of ground reflectivity and topography on erythemal UV radiation on inclined planes*, Int J Biometeorol, **46**, 95–104.

Willmott, C. J., 1982: *On the climatic optimization of the tilt and azimuth of flat-plate solar collectors*, Sol Energy, **28**, 205–216.

Willmott, C. J. and Matsuura, K., 2005: *Advantages of the mean absolute error (MAE) over the root mean square error (RMSE) in assessing average model performance*, Clim Res, **30**, 79–82.